UNIVERSITY OF SASKATCHEWAN
Subatomic Physics Institute
COLLEGE OF ARTS AND SCIENCE
NUCLEUS.USASK.CA/SPIN

Mass Predictions of Open-Flavour Hybrid Mesons from QCD Sum Rules

J. Ho, D. Harnett, T. G. Steele

Department of Physics & Engineering Physics

Affiliation:
University of Saskatchewan
Saskatoon, SK, Canada
Email: j.ho@usask.ca

Introduction

The seminal application of QCD sum-rules to heavy-light hybrids was performed by Govaerts, Reinders, and Weyers [6] (hereafter referred to as GRW). Therein, they considered four distinct currents covering $J \in \{0,\, 1\}$ in an effort to compute a comprehensive collection of ground state hybrid masses. Their correlator calculations took into account perturbation theory as well as 3d quark and 4d gluon condensate contributions, and precisely half of the channels yielded proper mass predictions. However, for all heavy-light hybrids, the square of the ground state hybrid mass was uncomfortably close to the continuum threshold (with a typical separation of roughly 100–200 MeV^2), and it was noted that even a modest hadron width would result in the resonance essentially merging with the continuum.

We extend the work of GRW by including both 5d mixed and 6d gluon condensate contributions in our correlator calculations. As noted in GRW, for heavy-light hybrids, condensates involving light quarks are multiplied by a heavy quark mass allowing for the possibility of a numerically significant contribution to the correlator and to the sum-rules. By this reasoning, the 5d mixed condensate could be a significant component of a QCD sum-rules application to the hybrid systems under consideration. As for the 6d gluon condensate, recent sum-rules analyses of closed, heavy hybrids [3] have demonstrated that it is important and can have a stabilizing effect on what were, in the pioneering work [5, 6, 4], unstable analyses.

Currents and Correlators

Following GRW, we define open hybrid interpolating currents

$$j_\mu = \frac{g_s}{2}\overline{Q}\Gamma^\rho\lambda^a q\mathcal{G}^a_{\mu\rho} \tag{1}$$

where g_s is the strong coupling and λ^a are the Gell-Mann matrices. The field Q represents a heavy charm or bottom quark with mass M_Q whereas q represents a light up, down, or strange quark with mass m_q. The Dirac matrix Γ^ρ satisfies (2) and the tensor $\mathcal{G}^a_{\mu\rho}$, the portion of (1) containing the gluonic degrees of freedom, satisfies (3) where $G^a_{\mu\rho}$ is the gluon field strength and $\tilde{G}^a_{\mu\rho}$ is its dual defined using the totally antisymmetric Levi-Civita symbol $\epsilon_{\mu\rho\nu\sigma}$.

$$\Gamma^\rho \in \{\gamma^\rho,\, \gamma^\rho\gamma_5\}, \tag{2}$$

$$\mathcal{G}^a_{\mu\rho} \in \{G^a_{\mu\rho},\, \tilde{G}^a_{\mu\rho} = \frac{1}{2}\epsilon_{\mu\rho\nu\sigma}G^a_{\nu\sigma}\} \tag{3}$$

For each of the four currents defined through (1)–(3), we consider a corresponding diagonal, two-point correlation function

$$\Pi_{\mu\nu}(q) = i\int \mathrm{d}^4x e^{iq\cdot x}\langle\Omega|\tau j_\mu(x)j^\dagger_\nu(0)|\Omega\rangle = \frac{q_\mu q_\nu}{q^2}\Pi^{(0)}(q^2) + \left(\frac{q_\mu q_\nu}{q^2} - g_{\mu\nu}\right)\Pi^{(1)}(q^2). \tag{4}$$

The tensor decomposition in (4) is such that $\Pi^{(0)}$ probes spin-0 states while $\Pi^{(1)}$ probes spin-1 states. Furthermore, each of $\Pi^{(0)}$ and $\Pi^{(1)}$ couples to a particular parity value. In the case of closed flavor hybrids, they also couple to a particular C-parity value, but, for open hybrids, this is not the case. For convenience, we will reference each of the $\Pi^{(0)}$ and $\Pi^{(1)}$ according to the J^{PC} combination it would have were we investigating closed rather than open hybrids; however, to stress that the C-value can not be taken literally, we will enclose it in brackets.

Γ^ρ	$\mathcal{G}^a_{\mu\rho}$	$J^{P(C)}$
γ^ρ	$G^a_{\mu\rho}$	$0^{+(+)},\ 1^{-(+)}$
γ^ρ	$\tilde{G}^a_{\mu\rho}$	$0^{-(+)},\ 1^{+(+)}$
$\gamma^\rho\gamma_5$	$G^a_{\mu\rho}$	$0^{-(-)},\ 1^{+(-)}$
$\gamma^\rho\gamma_5$	$\tilde{G}^a_{\mu\rho}$	$0^{+(-)},\ 1^{-(-)}$

Table 1: The $J^{P(C)}$ combinations probed through different choices of Γ^ρ and $\mathcal{G}^a_{\mu\rho}$.

$$\langle\overline{q}q\rangle = \langle\overline{q}^\alpha_i q^\alpha_i\rangle \tag{5}$$

$$\langle\alpha G^2\rangle = \langle\alpha_s G^a_{\mu\nu}G^a_{\mu\nu}\rangle \tag{6}$$

$$\langle g\overline{q}\sigma Gq\rangle = \langle g_s\overline{q}^\alpha_i\sigma^{\mu\nu}_{ij}\lambda^a_{\alpha\beta}G^a_{\mu\nu}q^\beta_j\rangle \tag{7}$$

$$\langle g^3G^3\rangle = \langle g_s^3 f^{abc}G^a_{\mu\nu}G^b_{\nu\rho}G^c_{\rho\mu}\rangle. \tag{8}$$

We calculate the correlators (4) within the operator product expansion (OPE) in which perturbation theory is supplemented by a collection of non-perturbative terms, each of which is the product of a perturbatively computed Wilson coefficient and a non-zero vacuum expectation value (VEV) or condensate. We include condensates up to and including those of dimension (d) six:

where the VEVs (5)–(8) are respectively referred to as the 3d quark condensate, the 4d gluon condensate, the 5d mixed condensate, and the 6d gluon condensate.

The Wilson coefficients (including perturbation theory) are computed to leading-order (LO) in g_s using coordinate-space, fixed-point gauge techniques (see [1], for example). Light quark masses are included in perturbation theory through a light quark mass expansion, but have been set to zero in all other OPE terms. The contributing Feynman diagrams are depicted in Figure 1 (all Feynman diagrams are drawn using JaxoDraw [2]). where we follow as closely as possible the labeling scheme of [7]. (Note that there is no Diagram IV in Figure 1 because, in [7], Diagram IV corresponds to an OPE contribution stemming from 6d quark condensates.) Divergent integrals are handled using dimensional regularization in $D = 4 + 2\epsilon$ spacetime dimensions at a renormalization scale μ^2, and we use the program TARCER [8] to reduce complicated, two-loop integrals to a small collection of simple basic integrals, all of which are well-known for the diagrams under consideration.

Sum Rule Methodology

Based on their dimension and analytic properties when viewed as a function of $Q^2 = -q^2$, the functions $\Pi^{(0)}$ and $\Pi^{(1)}$ from (4) both satisfy a dispersion relation

$$\Pi(Q^2) = \frac{Q^8}{\pi}\int_{M_Q^2}^\infty \frac{\mathrm{Im}\Pi(t)}{t^4(t+Q^2)}\mathrm{d}t + \cdots,\ Q^2 > 0 \tag{9}$$

where the $\cdots$ represents subtractions constants, collectively a third degree polynomial in Q^2. The quantity Π on the left-hand side of (9) is to be identified with the OPE result, an expression written in terms of the parameters of QCD, namely the strong coupling, the quark masses, and the condensates. On the other hand, the quantity $\mathrm{Im}\Pi$ on the right-hand side of (9), known as the hadronic spectral function, contains the peaks which are identified with strong resonances; as such, it depends on hadronic paramaters such as masses, widths, and resonance coupling strengths. Therefore, the dispersion relation (9) serves to relate hadronic parameters to QCD parameters, and, in principle, could be used to extract properties of hadrons directly from QCD.

We introduce the Borel transform

$$\hat{\mathcal{B}} = \lim_{\substack{N,Q^2\to\infty \\ \tau = N/Q^2}} \frac{(-Q^2)^N}{\Gamma(N)}\left(\frac{d}{dQ^2}\right)^N \tag{10}$$

where the transform variable τ is called the Borel scale, and use it to define the k^{th}-order Laplace sum-rule (LSR)

$$\mathcal{R}_k(\tau) = \frac{1}{\tau}\hat{\mathcal{B}}\left\{(-Q^2)^k\Pi(Q^2)\right\} = \int_{M_Q^2}^\infty t^k e^{-t\tau}\frac{1}{\pi}\mathrm{Im}\Pi(t)\mathrm{d}t,\ k \geq 0, \tag{11}$$

considering the dispersion relation (9).

In a typical QCD sum-rules analysis, the hadronic spectral function is parametrized in terms of a small number of hadronic quantities, predictions for which are then extracted using some fitting procedure. In what follows, we employ the "single narrow resonance plus continuum" model

$$\frac{1}{\pi}\mathrm{Im}\Pi(t) = f_H^2 m_H^8\delta(t - m_H^2) + \theta(t - s_0)\frac{1}{\pi}\mathrm{Im}\Pi^{\mathsf{OPE}}(t) \tag{12}$$

where m_H is the ground state resonance mass, f_H is its coupling strength, θ is a Heaviside step function, s_0 is the continuum threshold parameter, and $\mathrm{Im}\Pi^{\mathsf{OPE}}$ is the imaginary part of the expression for Π. Substituting (12) into (11) and defining subtracted LSRs by

$$\mathcal{R}_k(\tau,\, s_0) = \mathcal{R}_k(\tau) - \int_{s_0}^\infty t^k e^{-t\tau}\frac{1}{\pi}\mathrm{Im}\Pi^{\mathsf{OPE}}(t)\mathrm{d}t, \tag{13}$$

we find the result

$$\mathcal{R}_k(\tau,\, s_0) = f_H^2 m_H^{8+2k}e^{-m_H^2\tau} \Rightarrow \frac{\mathcal{R}_1(\tau,\, s_0)}{\mathcal{R}_0(\tau,\, s_0)} = m_H^2 \tag{14}$$

giving us the central equation of our analysis methodology.

To develop an OPE expression for $\mathcal{R}_k(\tau,\, s_0)$, we exploit a relationship between the Borel transform and the inverse Laplace transform $\hat{\mathcal{L}}^{-1}$ [9]:

$$\frac{1}{\tau}\hat{\mathcal{B}}\left\{f(Q^2)\right\} = \hat{\mathcal{L}}^{-1}\left\{f(Q^2)\right\} = \frac{1}{2\pi i}\int_{c-i\infty}^{c+i\infty} f(Q^2)e^{Q^2\tau}\mathrm{d}Q^2 \tag{15}$$

where c is chosen such that $f(Q^2)$ is analytic to the right of the integration contour in the complex Q^2-plane. Then, applying definitions (11) and (14) to the correlator and making use of the identity (15), it is straightforward to show that

$$\mathcal{R}_0(\tau,\, s_0) = M_Q^2\int_1^{\frac{s_0}{M_Q^2}} e^{-xM_Q^2\tau}\frac{1}{\pi}\mathrm{Im}\Pi(xM_Q^2)\mathrm{d}x + \frac{e^{-M_Q^2\tau}M_Q^3\alpha_s\langle g\overline{q}\sigma Gq\rangle}{108\pi}\left[a\log\left(\frac{M_Q^2}{\mu^2}\right) + b\right],\ \{a,\, b\}\,\text{constant}. \tag{16}$$

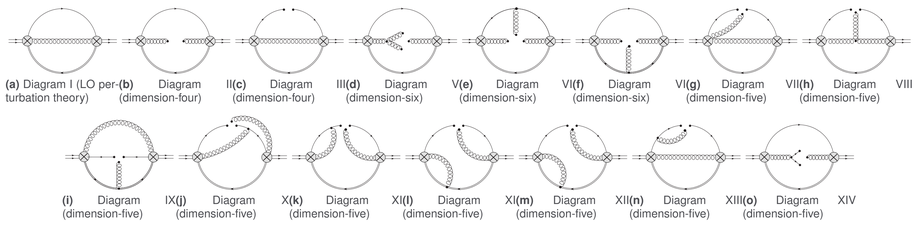

Figure 1: The Feynman diagrams contributing to the correlator. Single solid lines correspond to light quark propagators whereas double solid lines correspond to heavy quark propagators.

To extract stable mass predictions from the QCD sum-rule, we require a suitable range of values for our Borel scale (τ) within which our analysis can be considered reliable. Within this range, we perform a minimization procedure to obtain an optimized value of the continuum onset (s_0) associated with our resulting mass prediction. We determine the bounds of our Borel scale by examining two conditions: the convergence of the OPE, and the contribution of the pole mass to the overall mass prediction. We mirror our previous work done in charmonium and bottomonium systems [3]; to enforce OPE convergence and obtain an upper-bound on our Borel window (τ_{max}), we require that contributions to the dimension-four condensate be less than one-third that of the perturbative contribution, and the dimension-six gluon condensate contribute less than one-third of the dimension-four condensate contributions.

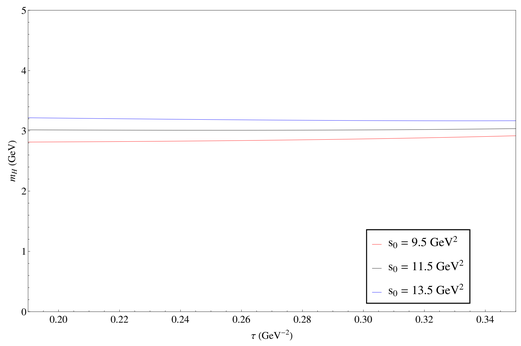

Figure 2: Illustrating the stability of mass predictions for $1^{-(-)}$ charm-light channel. The sum rule is plotted in the τ window for the optimized value of s_0 shown in black; the predictions for surrounding values of the continuum parameter have been included to demonstrate the insensitivity of the mass prediction to shifts in s_0. The stability of the mass in the predicted τ window demonstrates the viability of the prediction

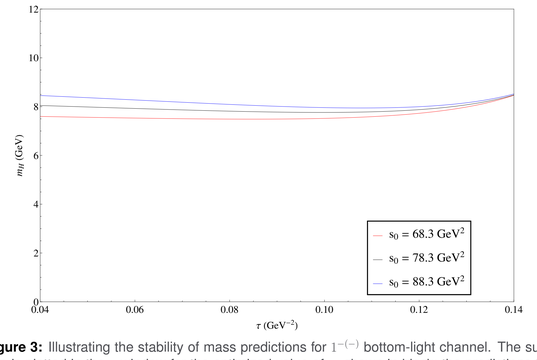

Figure 3: Illustrating the stability of mass predictions for $1^{-(-)}$ bottom-light channel. The sum rule is plotted in the τ window for the optimized value of s_0 shown in black; the predictions for surrounding values of the continuum parameter have been included to demonstrate the insensitivity of the mass prediction to shifts in s_0. The stability of the mass in the predicted τ window demonstrates the viability of the prediction

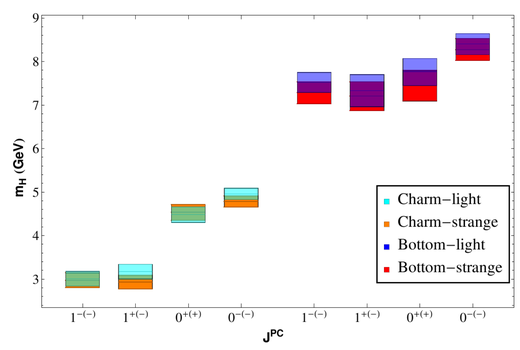

Figure 4: Summary of mass predictions with uncertainties for charm and bottom hybrid systems for the stabilizing $J^{P(C)}$ channels

Results

For each heavy-light hybrid combination under consideration, we performed a LSRs analysis of all eight distinct $J^{P(C)}$ combinations defined according to Table 1. As can be inferred from Figure 4 , half of the analyses stabilized; the other half did not. In particular, the $J^{P(C)} \in \{0^{+(+)}, 1^{-(-)}, 1^{+(-)}\}$ analyses were stable while the $J^{P(C)} \in \{0^{+(-)}, 1^{+(+)}, 1^{-(+)}\}$ were unstable. For charm-light and charm-strange hybrids, the $0^{-(-)}$ sector stabilized whereas the the $0^{-(+)}$ sector did not. For bottom-light and bottom-strange hybrids, this situation was reversed: the $0^{-(+)}$ sector stabilized while the the $0^{-(-)}$ sector did not. Note that, for all four heavy-light quark combinations considered, we did arrive at a unique mass prediction for each J^P. Within computational uncertainty, the mass spectra of the heavy-light hybrid systems are predicted to be degenerate with their heavy-strange counterparts. This is unsurprising given how numerically insignificant the light quark masses are to the hybrid LSRs under consideration, as (again) corrections to perturbation theory are largely driven by the 4d gluon condensate. In addition, the two spin-1 mass predictions are degenerate in the charm systems and are nearly so in the bottom systems. Furthermore, for charm hybrids, there is a large splitting between the spin-1 mass and the (mean) spin-0 mass with the spin-0 states coming in significantly heavier than the spin-1 states. For bottom hybrids, on the other hand, the relative splittings between states is much less pronounced than for charm hybrids.

Conclusions

In conclusion, we have presented predictions for the masses of charm-light, charm-strange, bottom-light, and bottom-strange hybrids for $J^P \in \{0^\pm,\ 1^\pm\}$ utilizing QCD sum-rules and improving upon the calculations of [5] by updating the non-perturbative parameters in the calculation, and including higher dimensional condensates in the OPE that have been shown important to sum-rule stability. We find a degeneracy in the heavy-light and heavy-strange states, and stabilization in the previously unstable $0^{-(-)}$ and $1^{-(+)}$ channels driven by the addition of the higher dimensional mixed and 6d gluon condensate contributions. As a consequence of these higher dimensional contributions, the $1^{+(+)}$ channel is destabilized from the original analysis of [5].

Acknowledgments

We are grateful for financial support from the Natural Sciences and Engineering Research Council of Canada (NSERC).

References

[1] E. Bagán, M. R. Ahmady, V. Elias, and T. G. Steele. plane-wave, coordinate-space, and moment techniques in the operator-product expansion: equivalence, improved methods, and the heavy quark expansion. *Zeitschrift fur Physik C: Particle Fields*, 61:157–170, 1994.

[2] D. Binosi and L. Theussl. Jaxodraw: A graphical user interface for drawing feynman diagrams. *Computer Physics Communications*, 161:76–86, 2004.

[3] Wei Chen, R. T. Kleiv, T.G. Steele, B. Bulthuis, D. Harnett, J. Ho, T. Richards, and Shi-Lin Zhu. Mass spectrum of heavy quarkonium hybrids. *Journal of High Energy Physics*, 1309:019, 2013.

[4] J. Govaerts, L. J. Reinders, P. Francken, X. Gonze, and J. Weyers. coupled QCD sum rules for hybrid mesons. *Nuclear Physics B*, 284:674, 1987.

[5] J. Govaerts, L. J. Reinders, H. R. Rubinstein, and J. Weyers. Hybrid quarkonia from QCD sum rules. *Nuclear Physics B*, 258:215, 1985.

[6] J. Govaerts, L. J. Reinders, and J. Weyers. Radial excitations and exotic mesons via QCD sum rules. *Nuclear Physics B*, 262:575, 1985.

[7] J. I. Latorre, P. Pascual, and S. Narison. spectra and hadronic couplings of light hermaphrodite mesons. *Zeitschrift fur Physik C: Particle Fields*, 34:347, 1987.

[8] R. Mertig and R. Scharf. TARCER - a Mathematica program for the reduction of two-loop propagator integrals. *Computer Physics Communications*, 111:265–273, 1998.

[9] M.Ā. Shifman, A.Ī. Vainshtein, and V.Ī. Zakharov. QCD and resonance physics. Theoretical foundations. *Nuclear Physics B*, 147:385, 1979.